

#### Journal of Advanced Scientific Research

Available online through <a href="https://sciensage.info">https://sciensage.info</a>

ISSN
0976-9595
Research Article

# PHYTONUTRIENT MEDIATED SYNTHESIS OF SILVER NANOPARTICLES FROM THE LEAF EXTRACT OF *MADHUCA LONGIFOLIA* (*KOENIG*) AND STUDY OF THEIR ANTIBACTERIAL EFFECTS

M. P. Somashekarappa\*, B. M. Naveena, B. S. Pragathi, S. Veena, U. Y. Mamatha, M. C. Kavya, N. Spoorthi
Department of PG Studies in Chemistry, IDSG College, Chikkamagaluru, Affiliated to Kuvempu University, Karnataka State, India
\*Corresponding author: psshekarl@rediffmail.com

Received: 04-12-2021; Revised: 01-03-2022; Accepted: 08-03-2022; Published: 31-03-2022

© Creative Commons Attribution-NonCommercial-NoDerivatives 4.0 International License

https://doi.org/10.55218/JASR.202213212

#### **ABSTRACT**

Silver nanoparticles (AgNPs) were synthesized using the aqueous extract of leaf of *Madhuca longifolia*. The particles were characterized using Uv-visible extinction spectroscopy, scanning electron microscopy (SEM), transmission electron microscopy (TEM) and powder X-ray diffraction (PXRD) studies. The average size of the AgNPs worked out using TEM and PXRD data were found to be 20-22 nm. Structure of the silver in their nanoparticles is found to be face centred cubic. Effect of the nanoparticles against the growth of *Escherichia coli (E. coli)* and *Staphylococcuus aureus (S. aureus)* were determined and compared with reference antibacterial substance ciprofloxacin. The AgNPs inhibit the spread of *E. coli* and *S. aurous* bacteria to different extents with their zones of inhibition 12 mm and 13.5 mm respectively.

**Keywords:** Antibacterial activity, *Escherichia coli*, *Maduca longifolia*, Silver nanoparticles, *Staphylococcus aureus*.

#### 1. INTRODUCTION

Thousands of remarkable industrial applications of the nanomaterials are due to their special and size dependant physico-chemical properties [1]. Properties and performance of the devices fabricated from the nanomaterials depends on the size, shape, structure, and the stability of the devices.

Silver nanoparticles (AgNPs) have been extensively explored class of nanomaterials for various applications owing mainly to their size, shape and structure dependant, surface plasmon resonance [2]. Areas of the applications of the silver nanoparticles include photocatalysis [3], optical sensors [4], nanosphere lithography [5], optoelectronics [6], solar energy conversion devices [7] and surface-enhanced Raman scattering (SERS) substrates [8]. Silver nanoparticles are also known for remarkable antimicrobial activities [9]. Representative precedents of the review of biomedical applications are mentioned here for reference [10-12]. The best known technical applications of the antimicrobial properties of the AgNPs are polyurethane based antibacterial water filter [13], AgNP impregnated blotting paper based point-to-use antibacterial water filter [14,15], activated carbon based antibacterial air filter [16] and AgNP embedded textile fabrics with antibacterial properties [17-20].

Chemical reduction methods using reducing agents such as NaBH<sub>4</sub>, LiAlH<sub>4</sub>, R<sub>4</sub>N<sup>+</sup>(Et<sub>3</sub>BH<sup>-</sup>) or hydrazine [21], results in unstable AgNP solutions contaminated with reaction by-products such as borides, metal borates [22], B<sub>2</sub>H<sub>6</sub>, NaNO<sub>3</sub> etc. Stabilizing the AgNPs in their solutions involves the use of various stabilizing agents [23], certain polymers, and cationic polynorbornenes [24], which makes the synthesis and stabilization expensive. In addition, the process will be multistep one. The synthesis of AgNPs by using mixed-valence polyoxometallates, polysaccharide, Tollens irradiation and biological methods have been regarded as greener approaches [25]. However, AgNP synthesis using aqueous extracts of plants is both greener and cheaper method in recent years [26, 27]. It has also been established that the sensitivity of AgNPs synthesized from plant extracts, for biosensing of fungicide and photocatalytic properties are relatively better [28].

Madhuka longifolia (Koenig), a very important medicinal plant grows in whole of India, is very much used for ethnomedical applications [29, 30]. This plant is been evaluated by researchers to be rich in bioactive constituents and fatty acids [31, 32], and oils that could be used as source of bio-energy [33]. In addition, seed extracts of Madhuca longifolia were used for fabrication of saponin-loaded silver nanoparticles [34] and

flavonoid-loaded silver, gold, silver-gold bimetallic nanoparticles [35] for the enhancement of antiinflamatory and wound healing bio-efficasies respectively. The synthetic method used was ultrasonication. Flower extract of this remarkably interesting plant has been used for the synthesis of AgNPs [36]. However, synthesis of AgNPs from the aqueous leaf extract of *Madhuca longifolia* has not been reported. Therefore in the present work we report the synthesis of AgNPs from the leaf extract of *Madhuca longifolia*, their characterization by Uv-visible extinction spectroscopy, powder X-ray diffraction, SEM and TEM analysis, and the study of their antibacterial activities against gram positive and gram negative bacteria.

#### 2. MATERIAL AND METHODS

#### 2.1. Material

The chemicals were from Merck, Himedia or from S. D. Fine chemicals. Distilled water was used throughout the experiments. Bacteria selected for the study were *E. coli and S. aureus*. A laboratory centrifuge, R-8C from Remi was used for isolation of particles for SEM and powder XRD analyses. Systronics Uv-visible spectrophotometer 119 was used for recording the Uv-visible extinction spectra in the wavelength range of 300 nm to 700 nm. Powder XRD patterns were recorded on a Rigacu Smartlab X-Ray diffractometer and the SEM and EDS were recorded on Ultra 55 scanning electron microscope from GEMINI technology. TEM imaging of the drop coated samples were done on Titan Themis 300kV from FEI.

#### 2.2. Methods

# 2.2.1. Extraction

Weighed quantities of the fresh leaves, were crushed in to paste with a little amount of warm distilled water using mortar and pestle. The paste was transferred in to a 250 mL beaker, suspended in 100mL water, stirred on a magnetic stirrer for about 30 minutes at 45-50°C temperature, cooled to lab temperature and filtered through a pre-weighed piece of qualitative filter paper. The weight of the contents transferred to the extract was calculated by difference in weight method. Qualitative phytochemical analysis of the extract was done following routine methods [37].

#### 2.2.2. Synthesis of Silver Nanoparticles

50 ml of the fresh extract containing approximately  $0.04\pm0.005~g/mL$  of extracted substances was taken in a round bottomed flask. Extract was heated to  $65^{\circ}C$  while stirring and 20mL of 0.002~M AgNO<sub>3</sub> solution

was added drop wise from a pressure equalizing dropping funnel for 20 minutes. During addition of silver nitrate solution, temperature was maintained at  $65\pm5^{\circ}$ C. Contents were stirred at  $65\pm5^{\circ}$ C for 2 hours and cooled to lab temperature. AgNP solution so obtained was centrifuged for isolation of the material, for powder XRD and SEM analyses. The samples were then dried in vacuum over anhydrous phosphorous pentoxide.

# 2.2.3. Antibacterial Activity Studies

The amount of AgNPs present in its solution was determined by evaporating known volume of AgNP solution on a pre-weighed watch glass, in to complete dryness and taking its weight. The difference in weight will give the amount of AgNPs present per unit volume of its solution. A solution of the reference substance, ciprofloxacin was prepared with the same concentration as that of AgNP solutions.

28 grams of nutrient agar was suspended in 1000 mL of distilled water and dissolved by boiling. The contents were autoclaved.

Fifteen mL aliquots of the nutrient agar media were transferred in to sterilized petri dishes. When the media hardened, the surface of the media was contaminated with bacteria using cotton swabs. The holes were scooped on the media and the holes were filled with different volumes of the AgNP solution and the solution of the reference substance. Petri dishes were incubated at 37°C for 20 hours. The zones of inhibition around the scooped holes were measured in mm.

#### 3. RESULTS AND DISCUSSION

Qualitative phytochemical analyses [37] were applied on the water extracts of the leaf samples with a total phytonutrient concentration of  $20 \times 10^{-3}$  g/mL. However, phytonutrient concentration used for AgNP synthesis ranges from  $8 \times 10^{-4}$  g/mL to  $40 \times 10^{-4}$  g/mL. Presence of phenolic compounds, flavonoides and saponines were confirmed reproducibly by the detailed phytochemical analyses, and the results are consistent with the reported literature [38] wherein authors have quantified twenty different phytochemicals by GC-MS and HPTLC methods.

Stability in all sizes and biocompatibility is an important requirement of the AgNPs to be applicable in biology and medicine [25]. However AgNPs synthesized using relatively harsh reducing agents such as sodium borohydride and without any stabilizing and capping molecules are unstable.

### 3.1. Synthesis

The present work describes the synthesis of stable AgNP solutions by using the water extract of *Madhuca longifolia* without any reducing agent and stabilizing molecules, and the method is highly reproducible. Most among twenty phytonutrient molecules present in the leaf extracts of the selected plant, as analysed by earlier reports belong the phenolic compounds and flavonoids which were identified qualitatively in this work. The drop wise addition of the AgNO<sub>3</sub> solution in to an extract containing the phytochemical molecules reduces the  $Ag^+$  in the  $AgNO_3$  in to atomic silver [27, 39-41] and hence the atoms condenses to nanosized particles. The particles are then instantaneously coated with bioactive molecules available in the solution to form a protective monolayer or multilayer [28, 42]. Particles coated with bioactive molecules in the solution, with the same surface properties get repelled by one another and hence exhibit good stability. The solutions are stable in the laboratory conditions for more than six months, and preparation of AgNPs by this method is highly reproducible.

# 3.2. Characterization

The Uv-visible extinction spectrum of the AgNPs synthesized using water extract of leaf sample of *Madhuca longifolia* is as shown in fig. 1(b).

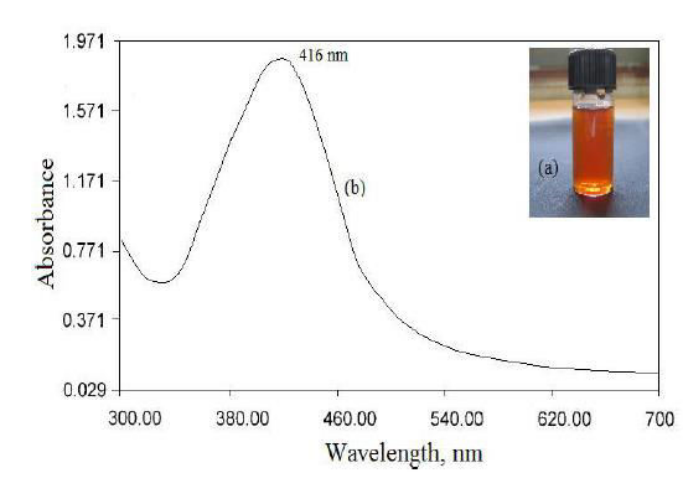
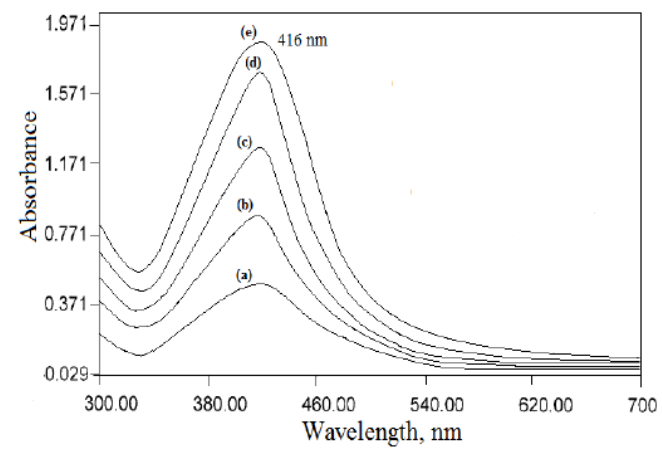


Fig. 1: (a) Colour of the AgNP solution and (b) Uv-visible extinction spectrum of the AgNPs synthesized from the extract of *Madhuca longifolia* 

Silver nanoparticles are characteristic of showing a surface plasmon resonance absorption band due to surface electrons, in the visible region of electromagnetic radiation [43, 44]. Though a change in colour from pale green to reddish brown as shown in

fig. 1(a), upon addition of AgNO<sub>3</sub> in to extract gives a visual indication of formation AgNPs, recording a uvvisible absorption spectrum in the region of 300-700 nm confirms the presence, approximate particle size and particle size distribution of AgNPs [45, 46]. Uv-visible spectrum recorded for the AgNPs absorption synthesized from the extract of Madhuca longifolia is given in fig. 1(b) and the data matches with that of the AgNPs obtained by reduction with hydrazine hydrate and with sodium citrate [47]. The  $\lambda_{max}$  is observed at 416 nm, and the spectrum recorded in the same wavelength range, for the extract alone did not show any absorption band. Thus uv-visible absorption band indicates the presence of AgNPs and its full width at half maximum (FWHM) represents approximate particle size distribution. Intensity of the absorption band and the  $\lambda_{max}$  did not change upon repeated recording of the spectrum of the same AgNP solution with regular intervals of one week and for a period of 60 days. This observation proves the good stability of the particles in their solution.

Two different sets of experiments were conducted to understand the dependence of particle size of the AgNPs on the concentration of the phytonutrients and on concentration of the AgNO $_3$  solution. Fig. 2 shows the Uv-visible extinction spectra recorded for the AgNP solutions obtained by adding  $2.0\times10^{-4}$  M AgNO $_3$  solution in to an extract of *Madhuca longifolia* with a phytonutrient concentration ranging from  $8\times10^{-4}$  g/mL to  $40\times10^{-4}$  g/mL.

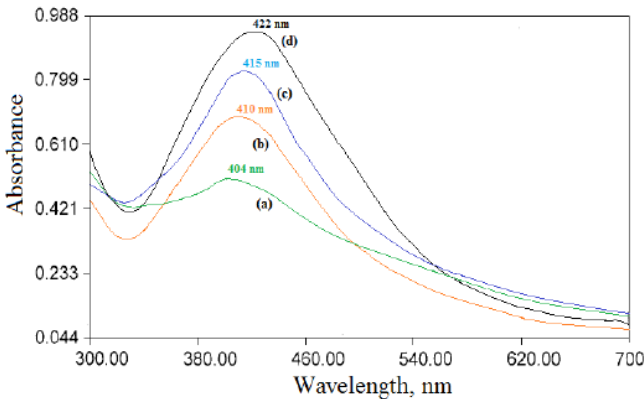


Solution prepared by adding  $2.0 \times 10^{-4}$  M AgNO<sub>3</sub> solution in to extracts of Madhuca longifolia, containing (a)  $8 \times 10^{-4}$  g/mL, (b)  $16 \times 10^{-4}$  g/mL, (c)  $24 \times 10^{-4}$  g/mL, (d)  $32 \times 10^{-4}$  g/mL, and (e)  $40 \times 10^{-4}$  g/mL of phytonutrients.

Fig. 2: Uv-visible absorption spectra of solution of the AgNP obtained by adding AgNO<sub>3</sub> solution in to extract of *Madhuca longifolia* with a varied phytonutrient concentration

Reaction of  $2.0 \times 10^{-4}$  M AgNO<sub>3</sub> solution with the extracts of Madhuca longifolia, having a phytonutrient concentration ranging from  $8 \times 10^{-4}$  g/mL, to  $40 \times 10^{-4}$ g/mL resulted in the AgNP solutions showing the same  $\lambda_{max}$  at 416 nm (fig. 2). However the increase in intensity of the Uv-visible absorption spectral band at 416 nm (fig. 2(a)-2(e)) indicates that, as the concentration of the phytonutrients increases, the yield or the concentration of the AgNPs increases. No change in the  $\lambda_{max}$  at 416 nm reveals that, the size of the AgNPs and their distribution is not affected by increase in concentration of extract.  $2.0 \times 10^{-4}$  M AgNO<sub>3</sub> solution is of sufficiently good concentration to yield AgNPs with size corresponding to a  $\lambda_{max}$  of 415-416 nm. As the concentration of the phytonutrients increases, reducing ability of the extract increases and thus the number or the concentration of the particles increases. The size of the particles is controlled by the concentration of the phytonutrient molecules acting as capping agents in order to stabilize them. Irrespective of the concentration of phytonutrients, particles are stabilized to the same size. This may be attributed to the fact that, adsorption of capping molecules upon the particles is so rapid so that as soon as particles are formed they are stabilized by capping.

Fig. 3 shows the uv-visible extinction spectra recorded for the AgNPs obtained by reacting an aqueous solution of fixed concentration ( $40\times10^{-4}$  g/mL) of phytonutrients, with an increased concentration of AgNO<sub>3</sub> from  $0.6\times10^{-4}$  M, to  $12\times10^{-4}$  M applying same reaction conditions.



Solution prepared by adding (a)  $0.6 \times 10^{-4}$  M, (b)  $1.4 \times 10^{-4}$  M, (c)  $2 \times 10^{-4}$  M and (d)  $12 \times 10^{-4}$  M AgNO<sub>3</sub> in to the extract of Madhuca longifolia containing  $40 \times 10^{-4}$  g/mL of phytonutrients

Fig. 3: Uv-visible absorption spectra of solution of the AgNP obtained by reacting solution of fixed concentration of phytonutrients, with an increased concentration of AgNO<sub>3</sub>

Experimental data obtained to check the dependence of particle size on the concentration of AgNO<sub>3</sub> given in fig. 3 revealed that, as the concentration of AgNO<sub>3</sub> lowered from  $2\times10^{-4}$  M to  $0.6\times10^{-4}$  M,  $\lambda_{max}$  decreases slightly to 404 nm (fig. 3a) through 410 nm (fig. 3b). Increasing the AgNO<sub>3</sub> concentration to  $12\times10^{-4}$  M (fig. 3d) from  $2 \times 10^{-4}$  M (fig. 3c),  $\lambda_{\text{max}}$  shows a slight increase to 422 nm. Considering the position of  $\lambda_{max}$  as a qualitative measure of particle size [45, 46] it is understood that an increase in concentration of AgNO3 at fixed constant concentration  $(40 \times 10^{-4} \text{ g/mL})$  of phytonutrients results in an increase in the particles size as indicated in fig. 3. This may be attributed to an increase in rate of reduction with respect to rise in AgNO<sub>3</sub> concentration. Morphology and the elemental composition of the AgNPs were understood using SEM and EDS data respectively, recorded on the AgNPs isolated by centrifugation at 4000 rpm from their solution having  $\lambda_{\text{max}}$  at 415-416 nm (fig. 1), are presented in fig. 4.

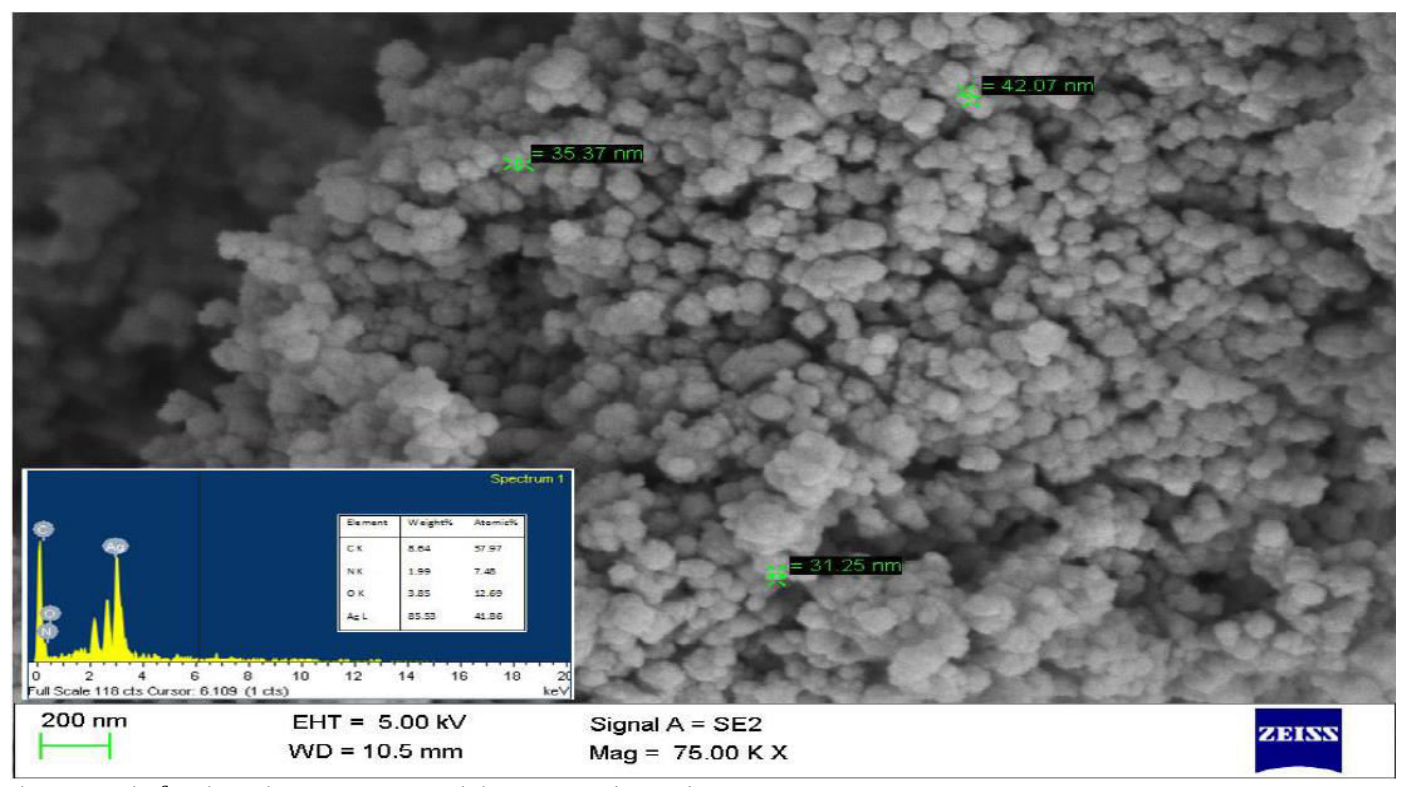
SEM image of the title material indicates that the spherical particles of AgNPs get agglomerated in to spherical lumps of various sizes ranging from 50 to 90 nm. Spherical agglomerates must have been formed during centrifugation. The AgNPs obtained by the present method consists of 85.53% Ag, 3.85% O, 1.99% N and 8.64% C as revealed by EDS profiling of expected elements (inset in fig. 4). Presence of oxygen, nitrogen and carbon is due to the involvement of organic molecules of plant origin in stabilizing the particles by forming a thin organic layer upon them.

TEM image recorded on the drop coated sample of AgNP solution is given in fig. 5. The inset in fig. 5 gives the particle size distribution worked out upon the TEM image.

The shapes of the AgNPs obtained by adopted method are spherical and quasi-spherical having higher percentage of the spherical particles as revealed by TEM imaging (fig. 5). The results are in fair consistency with those reported by earlier workers and few selective precedents could be referenced. Spherical AgNPs were synthesized using the extract of the plant, Terminalia bellirica [48]. AgNPs obtained by extracellular synthesis using Fungus, Aspergillus niger [49] were also spherical. However, AgNP synthesis using apiin as reducing agent [50] resulted in quasi-spherical particles. Analysis of averaged out particle size distribution using the TEM image reveals that the maximum particle size passes though 20 nm (inset in fig. 5). Relatively bigger and more uniformly spherical particles appeared in the SEM (fig. 4) compared to TEM picture are ascribable to

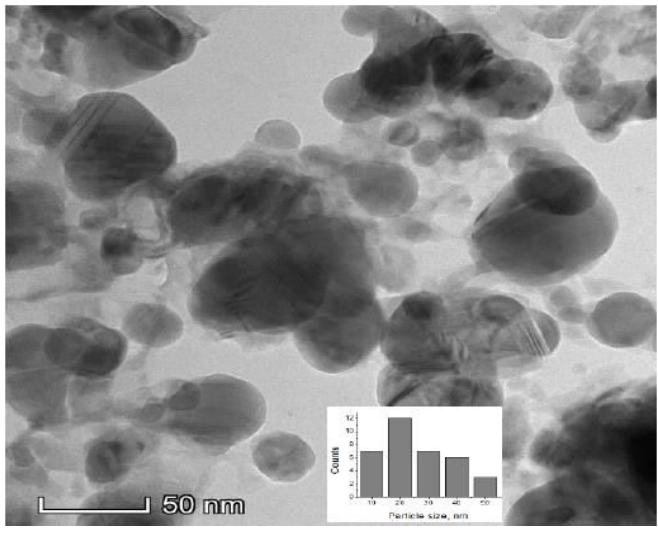
agglomeration of small and big particles having an organic molecular coating, in to bigger lumps of approximately 50-90 nm, during centrifugation and drying in vacuum.

Powder XRD pattern was recorded on the AgNP particles isolated by centrifugation in order to understand the crystal structure and the particle size. The pattern is presented in fig. 6.



The inset in the fig. shows the EDS spectrum and the respective elemental composition

Fig. 4: Scanning electron micrograph of AgNPs synthesized from the leaf extracts of Madhuca longifolia



Inset: Histogram showing the particle size distribution worked out upon TEM image

Fig. 5: Transmission electron mocrographs of the AgNPs synthesized from the extracts of Madhuka longifolia

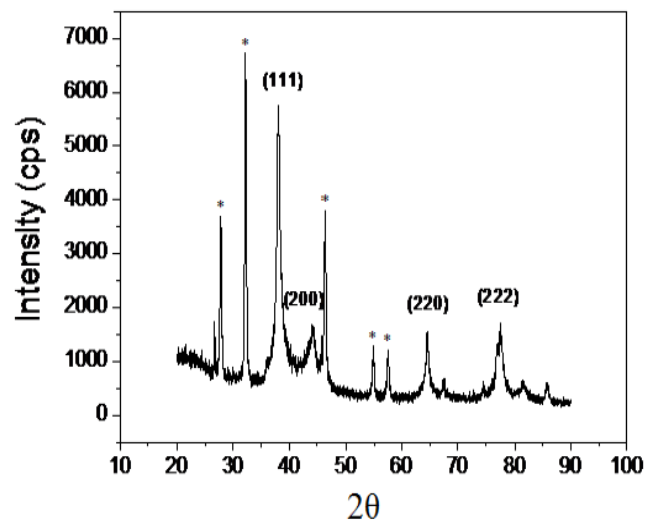


Fig. 6: Powder XRD pattern of AgNPs synthesized from the leaf extract of *Madhuka longifolia* 

Powder XRD pattern shows the presence of crystallographic planes (111), (200), (220), (222), and

indicative of the reduced silver by phytonutrients, being crystallized in to face centered cubic (FCC) structure. Relatively wider peaks in the PXRD pattern are characteristic of the material in the form of nanocrystallites. Average size of the particles is calculated using Debye-Scherer's formula D = 0.94  $\lambda/\beta$  $\cos \theta$ , where D is the average crystalline size,  $\lambda$  is the wavelength of X-ray,  $\beta$  is full width at half maximum and  $\theta$  is the angle of diffraction. The particle size of the AgNPs synthesized by the extract of Madhuca longifolia worked out with respect to (111) crystallographic plane is 22 nm. This value of particle size is consistent with the TEM results. The results of PXRD pattern are comparable with literature reports and consistent with the AgNPs prepared using aqueous extract of Ocimum Sanctum and quercetin (a flavonoid from the same plant) [51], root hair extract of *Phoenix dactylifera* [52], extracts of garlic, green tea and turmeric [53], extract of Sida cordifolia [54]. Some other sharp signals, marked by asterisk are shown in XRD pattern (fig. 7) may be ascribed to crystallization of any other phytonutrients which are not involved in reduction of AgNO<sub>3</sub>, or capping of the particles.

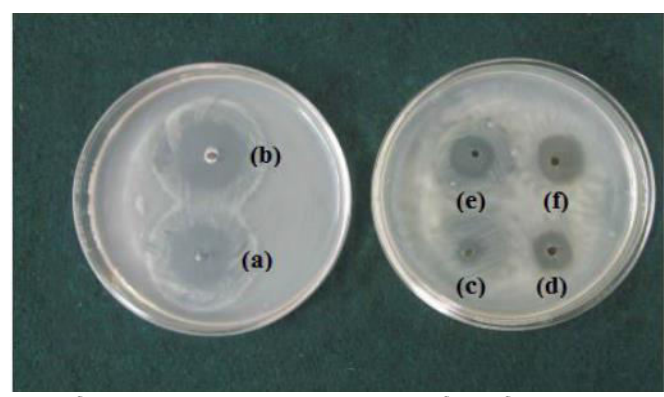
# 3.3. Antimicribial Activity Studies

Results of the comparative inhibitory effects of the AgNPs on the spreading of *E-coli* and against *S-aureus* bacteria, with respect to the reference compound, ciprofloxacin are shown in fig. 7 and fig. 8 respectively. Antimicrobial activity is an important characteristic property of silver nanoparticles [55]. The detailed reports on the studies of antimicrobial activities of the AgNPs were elaborately reviewed [56, 57].

In this study, as a representative application, the antibacterial properties of the AgNPs were checked against the growth of the *E. coli* and *S. aureus* bacteria by well diffusion method. The zones of inhibition against radial spread of the selected bacteria were determined for a period of 20 hours, conducting parallel experiments with a standard antibacterial substance ciprofloxacin.

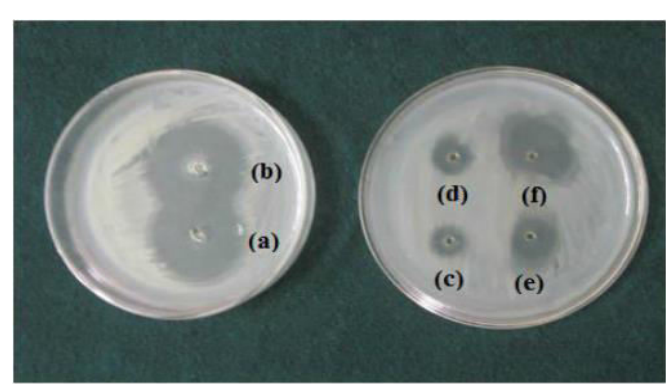
The AgNP solutions, diminishes the growth of both the bacteria selected for the study as indicated by a zone of inhibition around the wells filled with varied volumes of the AgNP solutions (fig. 7 and 8). It is clear that the zone of inhibition increases as the volume of AgNP solution in the well increases. The zones of inhibition obtained for the AgNPs prepared using the extract of *Madhuca longifolia* are 12.0 mm against the growth of *E. coli* (fig. 7(f)) and 13.5 mm against the growth *S. aureus* 

(fig. 8(f)). Patches (b) in both the fig. 7 and 8 are the zones of inhibition to the bacterial growth against 40 microliters of the suspension of reference substance and it is measured to be 13.5 mm against both *E. coli* and 15.0 mm against *S. aureus* bacteria respectively.



Holes filled with (a) 30  $\mu$ L and (b) 40  $\mu$ L of ciprofloxacin solution, and (c) 10  $\mu$ L, (d) 20  $\mu$ L, (e) 30  $\mu$ L (f) 40  $\mu$ L of AgNp solution prepared using water extract of Madhuca longifolia. Concencentration of AgNPs = 55  $\mu$ g/mL

# Fig. 7: Growth of *E-coli* bacteria around the scooped holes



Holes filled with (a) 30  $\mu$ L and (b) 40  $\mu$ L of ciprofloxacin solution, and (c) 10  $\mu$ L, (d) 20  $\mu$ L, (e) 30  $\mu$ L (f) 40  $\mu$ L of AgNp solution prepared using water extract of Madhuca longifolia. Concencentration = 55  $\mu$ g/mL

# Fig. 8: Growth of *S-aureus* bacteria around the scooped holes

### 4. CONCLUSION

Reacting an aqueous extract of the medicinal plant, *Madhuca longifolia* with silver nitrate solution at 65±5°C results in the formation of stable silver nanoparticles with an average particle size of 20-22 nm. The phytonutrients such as phenolic compounds, flavonoides and saponines present in the extract reduces the silver nitrate in to metallic silver and the metal so formed crystallizes in to FCC structure in the form of spherical

and quasi-spherical particles. AgNP solutions are highly stable because of the formation of a monomolecular layer on the surface of the particles. As the concentration of the phytonutrients increases, reducing ability of the extract and hence the yield of the particles increases. However, increase in concentration of AgNO<sub>3</sub> at fixed constant concentration of phytonutrients results in an increase in the particles size. The antibacterial properties of the AgNPs were checked against the growth of the E. coli and S. aureus bacteria by well diffusion method. The AgNP solutions, suppresses the growth of both the bacteria, with the determined zones of inhibition of 12.0 mm against of E. coli, and 13.5 mm against S. aureus respectively. Present study describes an easier, cheper and greener method for synthesis of AgNPs which uses a very common and useful medicinal plant species. Studies intended to understand the adsorption of these green synthesized AgNPs on various conducting and non conducting substrates will be of interest as the freshly prepared AgNPs are coated with phytonutrient molecules.

#### 5. ACKNOWLEDGEMENTS

Authors thank VGST for awarding a K-FIST level-1 grant which was used to establish basic laboratory facility. Author also thank Micro and Nano characterization facility, Center for nanoscience and engineering, IISc., Bangalore for extending characterization support under INUP programme. Authors also thank Dr. B. Thippeswamy, department of Microbiology, Kuvempu University for giving bacteria. This research did not receive any specific grant from funding agencies in the public, commercial, or not-for-profit sectors.

# Conflict of interest

Authors declare that they have no conflicts of interest.

#### 6. REFERENCES

- 1. Stark WJ, Stoessel PR, Wohlleben W, Haffner A. *Chem Soc Rev*, 2015; 44:5793-5905.
- 2. Amendola V, Bakr OM, Stellacci F. *Plasmonics*, 2010; **5:**85-97.
- 3. Awazu K, Fujimaki M, Rockstuhl C, Tominaga J, et al. *J Am Chem Soc*, 2008; **130**:1676-1680.
- McFarland AD, Van Duyene RP. Nano Lett, 2003;
   3:1057-1062.
- 5. Jensen TR, Malinsky MD, Haynes CL, Van. Duyne RP. *J Phys Chem B*, 2000; **104**:10549-10556.
- 6. Ko SJ, Choi H, Lee W, Kim T, et al. *Energ Environ Sci*, 2013; **6**:1949-1955.

- 7. Morfa AJ, Rowlen KL. Appl Phys Lett, 2008; **92**: 013504.
- 8. Li W, Guo Y, Zhang P. J Phys Chem C, 2010; 114: 6413-6417.
- 9. Rai M, Yadav A, Gade A. Biotechnol Adv, 2009; 27: 76-83.
- 10. Wong KKY, Liu X. Med Chem Commun, 2010; 1: 125-131.
- 11. Prabhu S, Poulose EK. Int Nano Lett, 2012; 2:32.
- 12. Burdusel AC, Gherasim O, Grumezescu AM, Mogoanta L, et al. *Nanomaterials*, 2018; **8**:680-704.
- 13. Jain P, Pradeep T. Biotechnol Bioeng, 2005; 90:59.
- 14. Dankovick TA, Gray DG. Environ Sci Technol, 2011; 45: 1992-1998.
- 15. Praveena SM, Karuppaiah K, Than LTL. *Cellulose*, 2018; **25**:2647-2658.
- 16. Yoon KY, Byeon JH, Park CW, Hwang J. *Environ Sci Technol*, 2008; **42**:1251-1255.
- 17. Ravindra S, Mohan YM, Reddy NN, Raju KM. *Colloids Surf A:Physicochem Eng Asp*, 2010; **367**:31-40.
- 18. Song J, Kang H, Lee C, Hwang SH, et al. ACS Appl Mater Interfaces, 2012; 4:460-465.
- 19. Wu M, Ma B, Pan T, Chen S, et al. *Adv Functional Mater*, 2016; **26**:569-576.
- 20. Zhang S, Tang Y, Vlahovic B. Nanoscale Res Lett, 2016; 11:80.
- 21. Schmid G, Chi LF. Adv Mater, 1998; 10:515-526.
- 22. Glavee GN, Klabunde KJ, Sorensen CM, Hadjapanayis. *Langmuir*, 1992; 8:771-773.
- Garcia-Barrasa J, López-de-Luzuriaga JM, Monge M. Cent Eur J Chem, 2011; 9:7-19.
- 24. Baruah B, Gabriel GJ, Akbashey MJ, Booher ME. *Langmuir*, 2013; **29**:4225-4234.
- 25. Sharma VK, Yngard RA, Lin Y. Adv Colloid and Interface Sci, 2008; 145:83-96.
- 26. Mittal AK, Chisti Y, Banerjee UC. Biotechnol Adv, 2013; 31:346-356.
- 27. Rajeshkumar S, Bharath LV. *Chem-Biol Interactions*, 2017; **273**:219-227.
- 28. Alex KV, Pavai PT, Rugmini R, Shiva Prasad M, et al. *ACS Omega*, 2020; **5**:13123-13129.
- 29. Akshatha KN, Mahadeva Murthy S, Lakshmidevi N. *Int J Life Sci Pharma Res*, 2013; **3**:44-53.
- 30. Sinha J, Singh V, Singh J, Rai AK. *J Nutr Food Sci*, 2017; **7**:573.
- 31. Ramadan MF, Sharanabasappa G, Parmjyothi S, Seshagiri M, et al. *Eur Food Res Technol*, 2006; **222**:710-718.
- 32. Yadav S, Suneja P, Hussain Z, Abraham Z, et al. *Biomass Bioenergy*, 2011; **35**:1539-1544.
- 33. Abraham Z, Yadav S, Latha M, Mani S, et al. Genet

- Resour Crop Evol, 2010; 57:619-623.
- 34. Sharma M, Yadav S, Sreevastava MM, Ganesh N, et al. *Asian J Nanosci Mater*, 2018; 1:244-261.
- 35. Sharma M, Yadav S, Ganesh N, Sreevastava MM, et al. *Prog Biomater*, 2019; **8**:51-63.
- 36. Patil MP, Sing RD, Koli PB, Patil KT, et al. *Microb Pathog*, 2018; **121**:184-189.
- 37. Raaman N, *Phytochemical Techniques*, New India Publishing Agency, New Delhi, 2006.
- 38. Annalakshmi R, Mahalakshmi S, Charles A, Savariraj Sahayam. *Drug Invent Today*; 2013; **5**:76-80.
- 39. Mandal D, Kumar Dash S, Das B, Chattopadhyay S, et al. *Biomed. Pharmacother*, 2016; **83**:548-558.
- 40. Priya RS, Geetha D, Ramesh PS. *Ecotoxicol Environ Saf*, 2016; **134**:308-318.
- 41. Gopinath K, Kumaraguru S, Bhakyaraj K, Mohan S, et al. *Microb Pathog*, 2016; **101**:1-11.
- Garcia-Barrasa J, López-de-Luzuriaga JM, Monge M. Cent Eur J Chem, 2011; 9:7-19.
- 43. Taleb A, Petit C, Pileni MP. *J Phys Chem B*, 1998; **102**:2214-2220.
- 44. Nogin ov MA, Zhu G, Bahoura M, Adegoke J, et al. *Opt Lett*, 2006; **31**:3022-3024.
- 45. Paramelle D, Sadovoy A, Gorelik S, Free P, et al. *Analyst*, 2014; **139**:4855-4861.

- 46. Desai R, Mankad V, Gupta SK, Jha PK. Nanosci Nanotechnol Lett, 2012; 4:30 34.
- 47. Guzman MG, Dille J, Godet S. *Int J Chem Biomol Eng*, 2009; **2**:104-111.
- 48. Anand KKH, Mandal BK. Spectrochim Acta A Mol Biomol Spectrosc, 2015; 135:639-645.
- 49. Gade AK, Bonde P, Ingle AP, Marcato PD, et al. *J Biobased Mater Bioenergy*, 2008; **2(3)**:243-247.
- 50. Kasturi J, Veerapandian S, Rajendran N. *Colloids and Surfaces B:Biointerfaces*, 2009; **68(1):**55-60.
- 51. Jain S, Mehata MS. Scientific Reports, 2017; 7: Article 15867.
- 52. Oves M, Rauf MA, Qayyum S, Qari HA, et al. *Mater Sci Eng C*, 2018; **89:**429-443.
- 53. Selvan DA, Mahendran D, Senthil Kumar R, Rahiman AK. *J Photochem Photobiol B:Biol*, 2018; **180:** 243-252.
- 54. Pallela PNVK, Ummey S, Ruddaraju LK, Pammi SVN, et al. *Microb Pathog*, 2018; **124**: 63-69.
- 55. Xiu ZM, Zhang QB, Puppala HL, Colvin VL, et al. *Nano Lett*, 2012; **12(8):**4271-4275.
- 56. Le Ouay B, Stellacci F. Nanotoday, 2015; **10(3)**: 339-354.
- 57. Roy A, Bulut O, Some S, Mandal AK, et al. *RSC Adv*, 2019; **9:**2673-2702.